EFFECT OF GREYSCALE/PRINT DENSITY ON THE PROPERTIES OF HIGH SPEED SINTERED NYLON 12

Christopher James Noble†, Adam Ellis† & Neil Hopkinson†

†Department of Mechanical Engineering, The University of Sheffield, Sheffield, S1 3JD, UK.

Abstract

High Speed Sintering is an Additive Manufacturing process that creates parts by sintering using inkjet and infra-red lamp technology, rather than the laser systems employed in Laser Sintering. This research investigated the effects of altering the dosage of ink (greyscale/print density) on the properties of parts produced. A clear pattern emerges that shows a 'sweet spot' for correct dosage of ink to maximise properties. The work also shows that greyscale allows considerable control of part density that could lead to substantial reductions in part mass beyond those that may be achieved by conventional design optimisation approaches employed today.

Introduction

Additive Manufacturing (AM) is the 'process of joining materials to make objects from 3D model data, usually layer upon layer, as opposed to subtractive manufacturing methodologies' [1]. It is increasingly being used for the creation of functional end-use parts, having previously been limited to producing visual representations of concepts in rapid prototyping and producing moulds in rapid tooling [2]. The layer-by-layer approach of AM combined with printing directly from computer data eliminates the need for tooling, which allows for increased design freedom and potential geometric complexity [3]. This also allows for optimisation and consolidation of parts, as well as being particularly relevant for individually customised parts, with even low-volume builds being economically viable.

Laser Sintering (LS) is an AM process in which parts are built layer upon layer using a laser to sinter cross-sections of powdered materials. The thermal energy provided by the laser is sufficient to sinter the underlying powder. A fresh layer of powder is deposited over the sintered layer, and the process repeats until the three-dimensional part is complete. The part is then allowed to cool and post-processed, which involves cleaning the part to remove any remaining powder and any other desired finishing operations [4]. One of the biggest advantages of LS is that unlike other AM processes the powder bed is self-supporting, allowing for high levels of geometric complexity. It also gives relatively high mechanical properties, allowing its parts to be used in a wide range of applications.

High Speed Sintering (HSS) is a development of Laser Sintering, but using an inkjet printhead and an IR heater rather than a laser [5]. An ink containing an infra-red radiation absorbing material (RAM) is deposited onto preheated powder *via* the printhead, followed by an IR lamp which passes over the entire build area. The area deposited with RAM absorbs a greater amount of thermal energy than the rest of the build bed, enough to sinter the powder. The process then repeats, layer-by-layer until the part is complete. HSS shares many of its advantages with LS, but eliminates some of the drawbacks. The need for expensive lasers is eliminated, machine costs are reduced and there is an increase in machine productivity as HSS cycle time is

independent of the part dimensions. The process is also scalable via the addition of printheads and IR lamps in series.

The current industry standard powder is Nylon 12, a polyamide thermoplastic with a semi-crystalline structure, containing both crystalline and amorphous regions. It has been used in both LS and HSS for years, with a large processing window and relatively high mechanical properties [5]. It demonstrates a narrow melt temperature range and a low melt viscosity, meaning it can quickly reach the level of fluidity necessary for good fusion without excess energy being inputted [6].

Problem Definition

As HSS is itself novel little research has yet been performed to investigate how print density influences the mechanical properties of parts. As the amount of energy absorbed by the powder will correspond to the density of RAM, it is expected that print density will influence mechanical properties. To date, most work has used the maximum print density the machine is capable of, the purpose of this research was to assess the influence of print density of mechanical properties of High Speed Sintered parts.

Greyscale & Print Density

To affect print density, two approaches are possible. A true greyscale image or a dithered pattern. Greyscale offers complete coverage of the printed area with the level of greyscale is determined by the volume of the ink droplet. A dithered pattern is matrix of printed fully black dots and therefore does not cover the entire area, in this case the amount of ink deposited is determined by the spacing between dots, see **Figure 1**.

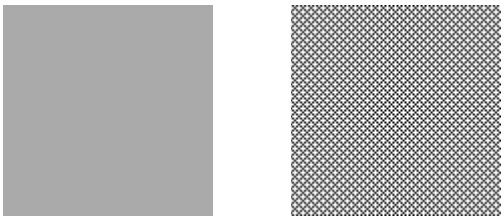

Figure 1: Greyscale (*left*) *vs.* dithering (*right*)

The Xaar Proton printhead used in the current HSS machine is only capable of printing in 1 bit, either a droplet is ejected or it is not. Thus, the current setup is not capable of printing variable droplet volumes. As such, a dithered pattern was used to determine print density rather than a true grayscale image.

Dithering is a way of converting 8-bit greyscale images to 1-bit monochrome images, where the various levels of grey in an 8-bit image are approximated *via* various densities of black dots in a 1-bit image [7]. Thus, a change in greyscale level in an 8-bit image corresponds to a change in dot density in a 1-bit image. The 8-bit scale ranges from black at 0 to white at 255,

therefore, the greyscale was first manipulated within this range and the subsequent grayscale image as converted into a dithered pattern as shown below in **Figure 2**.

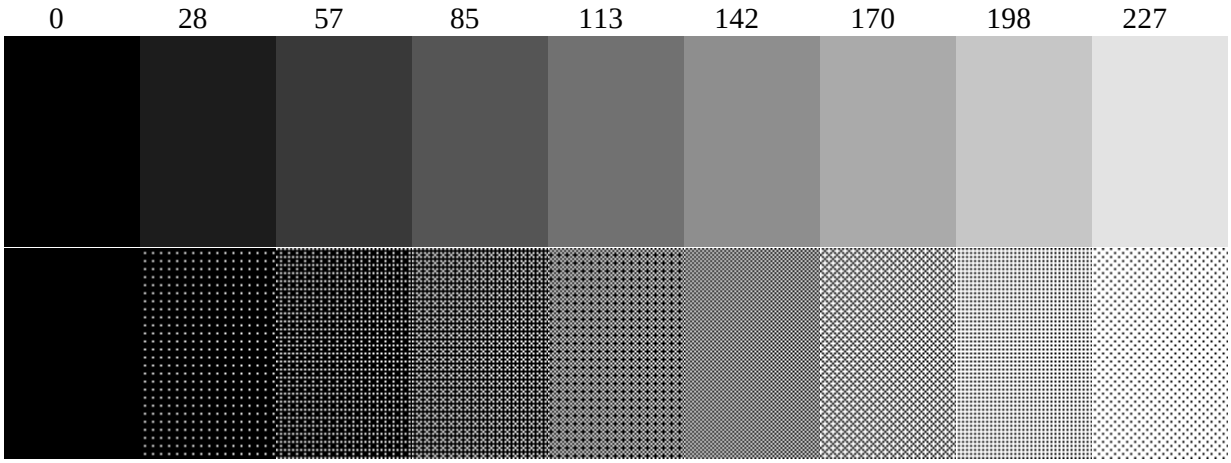

Figure 2: The process of creating dithered patterns with variable densities, the number above represents the level of grey scale with 0 as black and 227 as a light grey

This manipulation was performed using ImageJ, an open source java based image processing software. Dithering is based on an algorithm, of which many variations exist. Here the chosen algorithm was Bayer 4x4, as this yielded the most even density distribution.

Previous research in Laser Sintering has shown that larger particles often receive insufficient energy to fully melt, resulting in an unmolten particle core surrounded by melted and recrystallized material [8, 9]. This is evidenced by two distinct peaks in the Differential Scanning Calorimetry (DSC) curve, corresponding to melted and unmelted regions of the part, as seen in **Figure 3**. The amount of material which has melted and recrystallised gives the degree of particle melt (DPM). As print density corresponds to the amount of RAM deposited on the surface, it was anticipated that as the print density increased this would lead to an increased amount of energy absorbed and a higher DPM.

As also illustrated in **Figure 3**, the area under the DSC curve (mJ) may be derived, from which the heat of melting (J/g) can be calculated using the sample mass. The percentage crystallinity of the sample can then be calculated by comparing this value to that of a 100% crystalline sample, taken as 209.3 J/g based on research by Gogolewski *et al* [10].

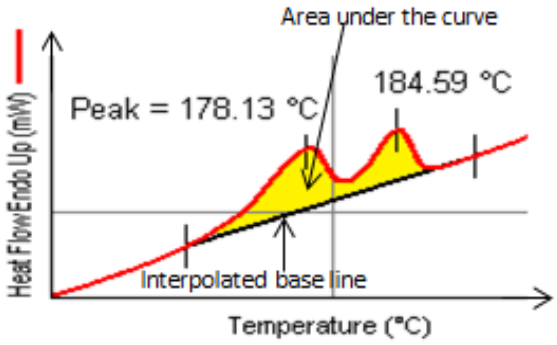

Figure 3: Analysis of a DSC trace

From this crystallinity value, the DPM can then be calculated, using **Equation 1**, as derived by Majewski *et al.* [11].

$$DPM = \frac{C_T - C_P}{C_{MR} - C_P} \qquad \textbf{Equation 1}$$

where C_P is the crystallinity of the powder (0.47) and C_{MR} is the crystallinity of the melted and recrystallised material (0.25) and C_T is the total crystallinity of the sample [11, 12].

An increase in DPM of parts also shows a corresponding decrease in total crystallinity, due to the melted and recrystallized material having a lower crystallinity than the un-melted material (25% *vs*. 47%). DPM is seen to increase, and percentage crystallinity decrease, as energy density (or energy per unit area) is increased, due to a greater amount of material receiving enough energy to melt and later re-crystallise [13]. However, even when the DPM is complete, an increase in energy density continues to give an apparent decrease in percentage crystallinity [11, 12]. This is thought to be due to excess energy causing degradation of the polymer chains, thus destroying the long-range order of the part and reducing its percentage crystallinity [14].

Previous work by Majewski *et al.* found that Ultimate Tensile Strength (UTS) increases with increasing energy density, due to a higher DPM, until the point where the DPM is complete, beyond which increasing energy causes a decrease in UTS values. For Elongation at Break (EaB), an increase is again seen with increasing energy density, followed by an apparent rise in EaB values at the point where the DPM is complete. No clear correlation has been found between Young's Modulus (YM) and energy density [11, 13].

Experimental Methodology

100% virgin Nylon 12 powder was used to manufacture 6 tensile specimens which conformed to ASTM D638-10, at the greyscale levels shown in **Table 1**. The machine parameters used are shown in **Table 2**.

Greyscale Levels	0	28	57	85	113	142	170	198	227

Table 1 - A table showing the greyscale levels used

Build Bed (°C)	Build overhead (°C)	Feed bed (°C)	Feed overhead (°C)	Preheat stroke (% @ mm/s)	Sintering stroke (% @ mm/s)
171	175	120	140	100 @ 170	100 @ 130

Table 2: The machine parameters used to build the tensile specimens

For density and DSC analysis, a rectangular block was also built between each set of tensile specimens. The layer thickness was 0.1 mm and the crystallinity and degree of particle melt calculated using methods described by Majewski *et al*.[11].

Tensile tests were carried out in accordance with ASTM D638-10 standards, using a Tinius Olsen H5KS Benchtop Materials Testing Machine, extruded at a rate of 5mm/min. A stress-strain curve was obtained for each of the specimens, an example is shown in **Figure 4.** The mechanical properties of interest were UTS, EaB and YM.

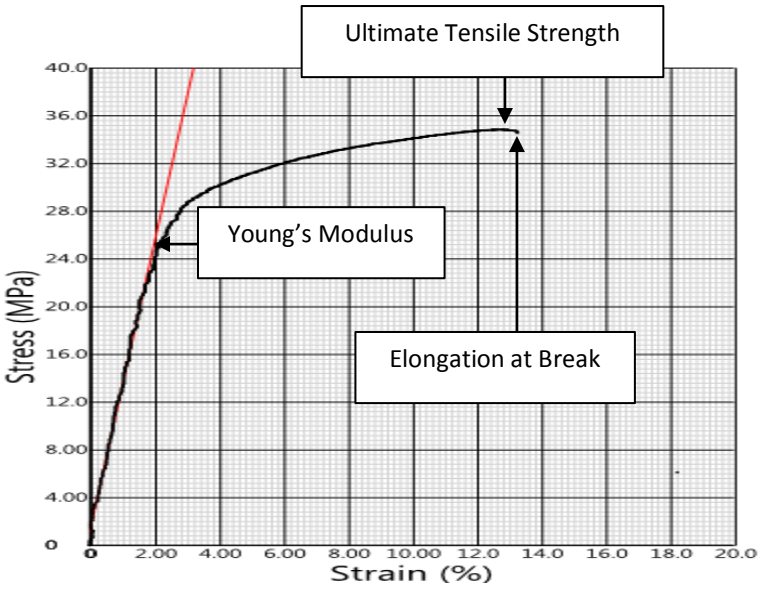

Figure 4: An example **s**tress strain curve produced by Tinius Olsen H5KS

Density of the samples was calculated by first obtaining the mass of each of the rectangular blocks, using an OHAUS Pioneer ™ PA64C analytical balance. A FARO Scan Arm 3D was then used to obtain a 3D scan of each of the blocks, as illustrated in **Figure 5**, from which part volume was obtained using Geomagic's Studio 3D scan processing software. The density of the parts was then simply mass divided by volume.

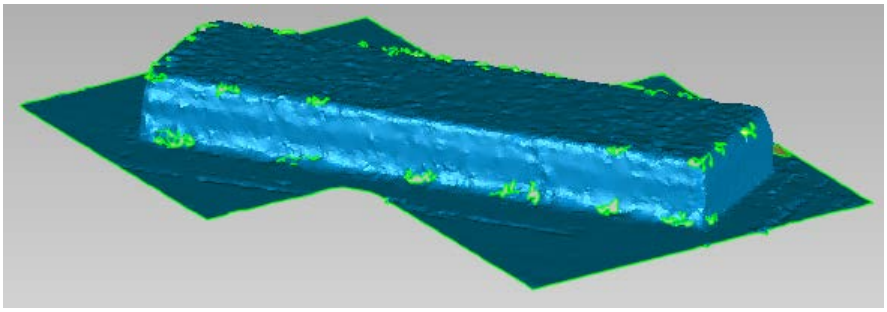

Figure 5: A typical 3D scan from the FARO Scan Arm 3D

DSC measurements were recorded using a Perkin Elmer DSC 8500 machine, and analysed using Pyris DSC analysis software. In accordance with previous work by Zarringhalam a 12mg sample (±3mg) was heated from 20^{o}C to 220 ^{o}C at a rate of 10 ^{o}C/min, before being held at 220 ^{o}C for two minutes, and then being cooled back down to 20^{o}C at the same rate of 10 ^{o}C/min. The samples were cut from the centre of each of the rectangular blocks [12].

Results and Discussion

Figure 6 shows how ultimate tensile strength is influenced by greyscale. It is important to note that a lower greyscale value indicates a higher print density.

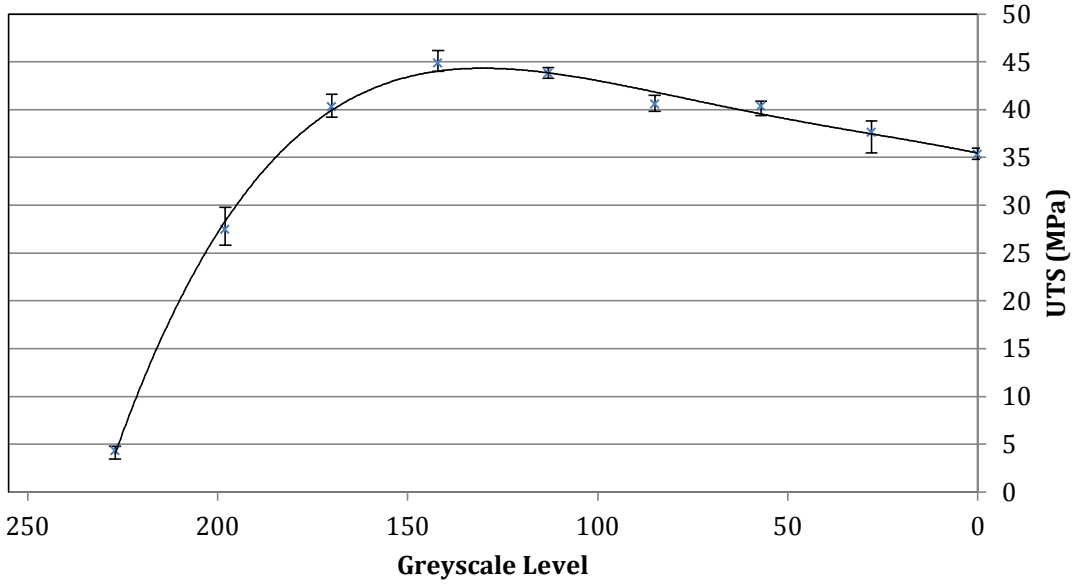

Figure 6: UTS *vs.* Greyscale Level

An increase in UTS is observed with a decrease in greyscale until the 142 greyscale level point. Beyond this, a decrease in UTS with decreasing greyscale was observed. The initial increase is likely to be due to a more complete fusion and better particle-to-particle contact, due to the increased energy absorbed due to more RAM. The decrease after the 142 greyscale level can be attributed to degradation of the polymer material and a likely decrease in part crystallinity, with lower crystallinity values associated with lower UTS values [15].

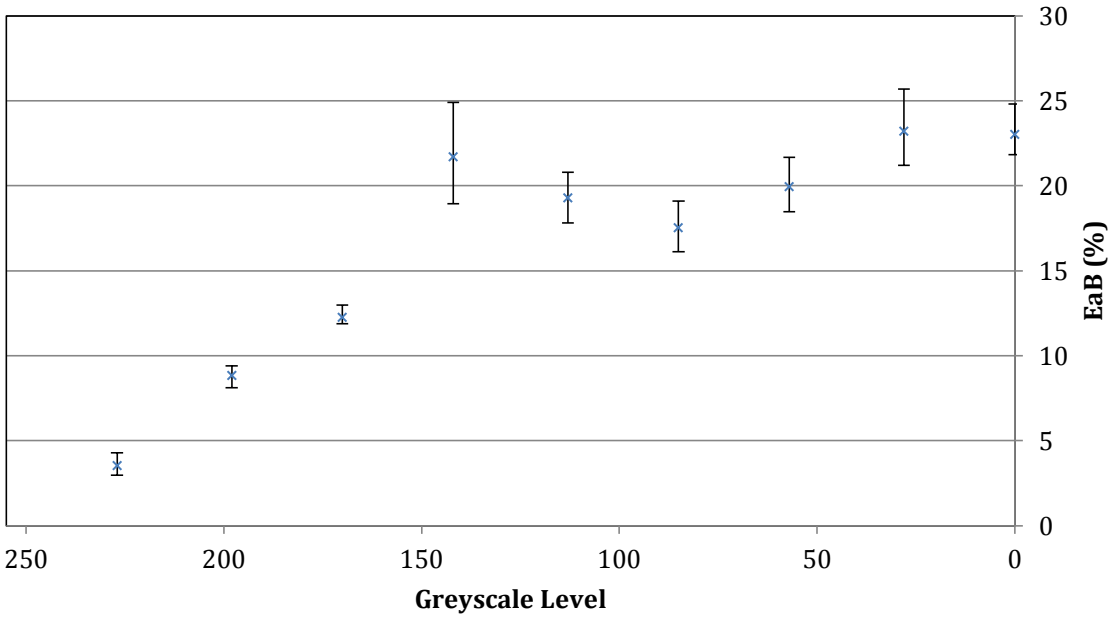

Figure 7: EaB *vs*. Greyscale Level

For EaB, as seen in **Figure 7,** a clear initial increase is observed once again, likely due to better fusion and particle-to-particle contact. There then appears to be a rise in EaB values around the 142 greyscale level, similar to results observed by Majewski *et al*. Beyond the 142 greyscale levels, a clear trend becomes harder to discern; it appears the results are broadly flat, with natural variations in the data.

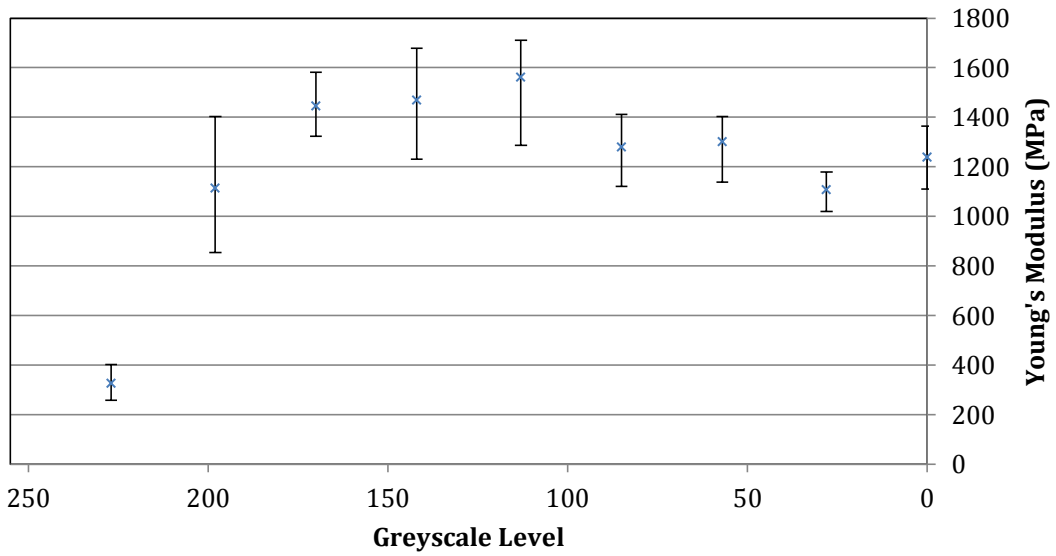

Figure 8: YM *vs.* Greyscale Level

For YM, an initial increase with decreasing greyscale can be observed in **Figure 8**, likely due to similar reasons as described previously. Beyond this however there is no clear trend, as expected based on previous research.

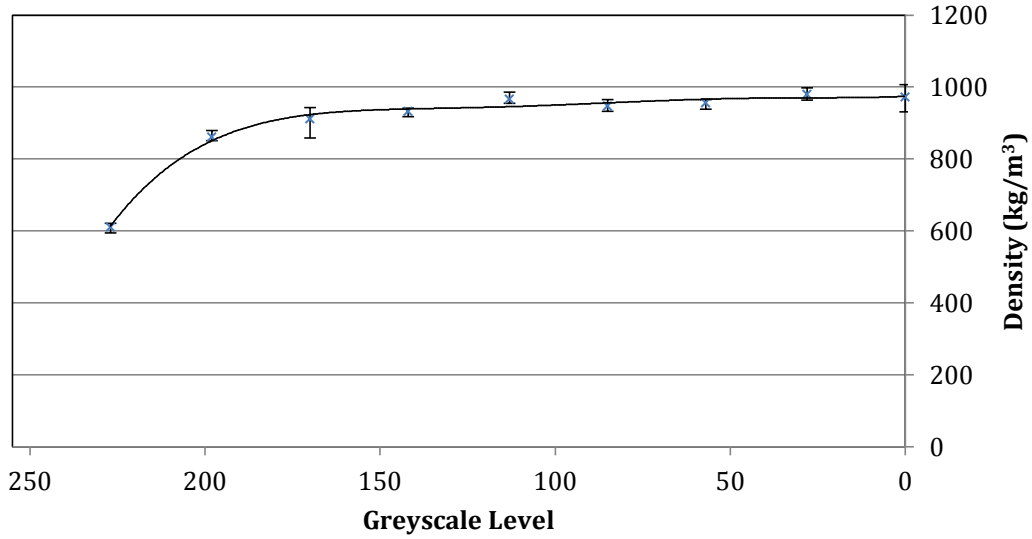

Figure 9: Density *vs.* Greyscale Level

In terms of part density, as seen in **Figure 9**, a sharp initial increase is seen with decreasing greyscale level, until the 170 greyscale level. Beyond this, the increase in density with decreasing greyscale is not so pronounced. This is likely due to the DPM being almost complete at this point, with any further energy just helping to close up any remaining pores. Combined

with the previous results, a clear potential can be seen to alter density of components whilst retaining acceptable mechanical properties.

Figure 10 shows the percentage crystallinity of each set of samples. As expected, a decrease in crystallinity with decreasing greyscale is seen, initially due to the greater amount of melted and recrystallized material, then due to degradation of the polymer chains destroying the long range order of the parts.

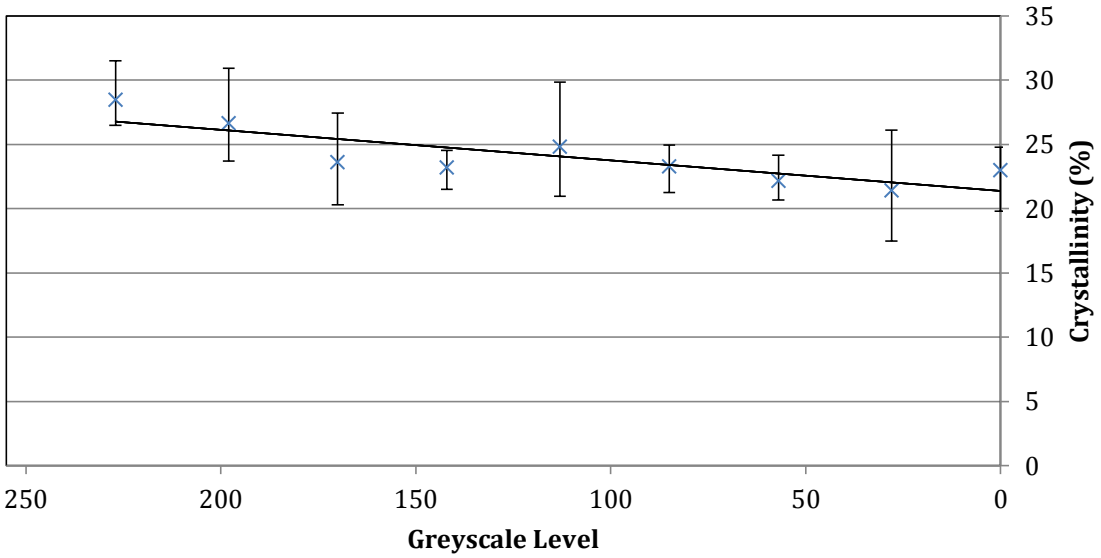

Figure 10: Crystallinity *vs*. Greyscale Level

From the crystallinity trendline, the DPM could be derived at each of the greyscale levels, giving the results seen in **Table 3**. The DPM appears to be complete somewhere between the 170 and 142 greyscale levels, which corresponds well with results seen previously; the highest UTS value was observed around the 142 greyscale level, and a jump in EaB occurred between 170 and 142. This is similar to the results observed by Majewski *et al*.

Greyscale Level	Derived DPM (%)
227	92.01
198	95.14
170	98.15
142	101.17
113	104.30
85	107.31
57	110.33
28	113.44
0	116.47

Table 3: The change in greyscale level *vs*. derived DPM

One interesting point to note is that the DPM continues to rise above 100%, which is clearly illogical. This is due to a fundamental limitation in Equation 2, whereby it is only valid for crystallinity values above the crystallinity of the melted and recrystallized region (25%). In practice, crystallinity can fall below this due to degradation of the polymer material. Therefore, **Equation 1** should be considered an identifier of where the DPM is complete, rather than as an exact calculation tool.

Conclusions

The experiments have shown that the amount of RAM has a significant effect on the properties of High Speed Sintered parts, with a decrease in greyscale/print density increasing the amount of thermal energy absorbed. The degree of particle melt at these parameters is complete around the 142 greyscale level, where maximum Ultimate Tensile Strength values were observed and very high relative values of Elongation at Break and Young's Modulus. The decrease in greyscale/print density also has a significant effect on density, possibly allowing for significant reductions in the mass of High Speed Sintered components.

References

1. Standard, A., *F2792. 2012. Standard Terminology for Additive Manufacturing Technologies.* ASTM F2792-10e1.
2. Wohlers, T., *Wohlers report 2012: state of the industry: annual worldwide progress report*. 2012: Wohlers Associates, Inc.
3. Hopkinson, N, Hague, R J M and Dickens, P M. *Rapid Manufacturing: An Industrial Revolution for the Digital Age*. Chichester : John Wiley & Sons, 2006. 978-0470016138.
4. Gibson, I., D.W. Rosen, and B. Stucker, *Additive Manufacturing Technologies*. 2010: Springer.
5. Thomas, H.R., N. Hopkinson, and P. Erasenthiran, *High Speed Sintering - Continuing Research into a New Rapid Manufacturing Process*, in *Solid Freeform Fabrication Symposium*. 2006: University of Texas, Austin, USA. p. 682-691.
6. Zarringhalam, H., et al., *Effects of processing on microstructure and properties of SLS Nylon 12*. Materials Science and Engineering: A, 2006. **435**: p. 172-180.
7. Miller, R., *Digital Art: Painting with Pixels*. 2007: Twenty-First Century Books.
8. Moeskops, E., N. Kamperman, and B. van de Vorst. *Creep behaviour of polyamide in selective laser sintering*. in *Proceedings of the 15th Solid Freeform Fabrication Symposium, .* 2004. University of Texas, Austin, USA.
9. Shi, Y., et al., *Effect of the properties of the polymer materials on the quality of selective laser sintering parts.* Proceedings of the Institution of Mechanical Engineers, Part L: Journal of Materials Design and Applications, 2004. **218**(3): p. 247-252.
10. Gogolewski, S., K. Czerntawska, and M. Gastorek, *Effect of annealing on thermal properties and crystalline structure of polyamides. Nylon 12 (polylaurolactam)*. Colloid and Polymer Science, 1980. **258**(10): p. 1130-1136.
11. Majewski, C., H. Zarringhalam, and N. Hopkinson. *Effects of Degree of Particle Melt and Crystallinity in SLS Nylon-12 Parts*. in *19th Solid Freeform Fabrication Symposium*. 2008. University of Texas, Austin, USA.
12. Zarringhalam, H., *Investigation into Crystallinity and Degree of Particle Melt in Selective Laser Sintering*. 2007, Loughborough University, UK.
13. Hopkinson, N., C. Majewski, and H. Zarringhalam, *Quantifying the degree of particle melt in Selective Laser Sintering®*. CIRP Annals-Manufacturing Technology, 2009. **58**(1): p. 197-200.
14. Vasquez, M., B. Haworth, and N. Hopkinson, *Optimum sintering region for laser sintered nylon-12*. Proceedings of the Institution of Mechanical Engineers, Part B: Journal of Engineering Manufacture, 2011. **225**(12): p. 2240-2248.
15. Flory, P.J., *Principles of polymer chemistry*. 1953: Cornell University Press.